Power Harmonic Component Suppression in case of Un-Ideal Electro-motive Forces

Paolo Meloni, Alessandro Serpi
Department of Electrical and Electronic Engineering
University of Cagliari
Cagliari, Italy

***Abstract*—A control system to suppress power Harmonic Components (HCs) when supplying an electric grid or motor characterized by un-ideal three-phase electro-motive forces (emfs) is presented in this paper. The proposed method can be applied in case of any three-phase emfs consisting of a certain number of HCs, each of which made up of positive-, negative-, and/or zero-sequence components. Based on emf features, different three-phase reference currents can be defined in accordance with the available degrees of freedom and power HC suppression targets. These reference currents are tracked by means of a deadbeat predictive current control algorithm, which is developed in the stationary reference frame to account for a possible wide and dense current harmonic spectrum. The effectiveness of the proposed solution is verified though a simulation study, whose results confirm the validity of the proposed theoretical approach.**

Keywords—Current control, Harmonic analysis, Power conversion harmonics, Predictive control

I. INTRODUCTION

Current control systems are widely employed for both electric drives and grid-connected power electronic converters in manifold applications [1], ranging from industrial drives and electric propulsion systems to renewable energy power plants and energy storage systems. A current control system must ensure an appropriate tracking of the reference currents, which can be either self-defined in accordance with given targets or inputted by a higher control level. Regarding electric drives, reference currents are generally defined in accordance with electromagnetic torque and magnetic flux needs, whereas they are generally enslaved to the required active and reactive power flow in case of grid-connected converters.

Regardless of the specific application, reference currents are defined in accordance with system model, which generally encloses a three-phase electro-motive force (emf). The latter can be either speed-dependant in case of an electric drive, or ideally constant in case of grid applications. The emf is also generally assumed characterised by just the fundamental positive-sequence harmonic component, especially for control system design purposes. However, un-ideal emfs generally occur, namely emfs characterised by different sequence and/or harmonic components caused by different phenomena [2]–[4]. In these cases, injecting ideal reference currents unavoidably leads to power Harmonic Components (HCs), which may cause excessive torque ripple (in case of electric drives) or power fluctuations (in case of grid applications).

Most of the literature focuses on suppressing and/or mitigating current HCs, especially in grid applications, e.g. [4]–[8]. However, there are some studies that address Power HC Suppression (PHCS) too. Particularly, power ripple due to un-ideal emfs is mitigated in [9]–[11], but without exploiting high-order current HCs. These are instead employed in [12] to achieve smooth active and reactive powers, by developing a current control system into the stationary reference frame. A similar approach is proposed in [13], but specifically referring to 5th- and 7th-order HCs so that a proportional-integral-resonant current controller can be employed in the synchronous reference frame.

In this context, a PHCS strategy is proposed in this paper. Differently from previous studies, the proposed methodology can be applied in presence of any three-phase emfs, whose features concur to determine the most suitable reference currents to inject. Additionally, the proposed strategy focuses on power rather than current HC suppression, namely different reference current profiles can be defined depending on number and kind of emf HCs (i.e., positive-, negative-, and/or zero-sequence components), as well as the desired PHCS targets. Once the reference currents have been defined, they are tracked by means of a deadbeat predictive current control algorithm, which has been developed in the stationary reference frame to ensure an appropriate tracking given the possible wide and dense current harmonic spectrum. The validity and effectiveness of the proposed approach has been tested through a simulation study, which has been carried out in MATLAB-Simulink and regards different cases and current profiles. The corresponding results confirm the proposed theoretical analysis, also showing some practical limitations and interesting future trends.

II. SYSTEM MODELLING

A. Phase quantities

A generic three-phase quantity u_x, be it a voltage, a current or a power, can be expressed as

$$u_x = \sum_{h=0} U_x^{(h)} \cos\left(h\left(\vartheta - \tfrac{2}{3}\pi\left(x-1\right)\right) - \varphi_x^{(h)}\right), \quad \vartheta = \omega t \quad (1)$$

in which $x \in \{1,2,3\}$ denotes the R, S, or T phase alternatively, $U^{(h)}$ and $\varphi^{(h)}$ are magnitude and angular displacement of the h-order harmonic component, while ϑ and ω are the grid voltage angle and fundamental angular frequency, respectively. Applying the Euler's formula to (1) yields

$$u_x = \tfrac{1}{2}\sum_{h=0}\left(u_x^{(h)} e^{-jh\frac{2}{3}\pi\left(x-1\right)} e^{jh\vartheta} + \overline{u}_x^{(h)} e^{jh\frac{2}{3}\pi\left(x-1\right)} e^{-jh\vartheta}\right) \quad (2)$$

in which $u_x^{(h)}$ denotes the h-order phasor of the phase x:

$$u_x^{(h)} = U_x^{(h)} e^{-jh\varphi_x^{(h)}} \quad (3)$$

while $\overline{\ }$ denotes the conjugate operator.

Still considering a three-phase system, the phase quantities can be combined to each other by means of the Clarke's transformation to achieve the corresponding space vector as

$$\begin{aligned} u_{\alpha\beta} &= u_\alpha + j u_\beta = \tfrac{2}{3}\left(u_1 + u_2\, e^{j\frac{2}{3}\pi} + u_3\, e^{j\frac{4}{3}\pi}\right) \\ u_\gamma &= \tfrac{1}{3}\left(u_1 + u_2 + u_3\right) \end{aligned} \quad (4)$$

in which the αβ components identify the well-known stationary reference frame, while γ denotes the zero-sequence component. Therefore, substituting (2) in (4) yields

$$\begin{aligned} u_{\alpha\beta} &= \sum_{h=0} u_{+}^{(h)} e^{jh\vartheta} + \sum_{h=0} u_{-}^{(h)} e^{-jh\vartheta} \\ u_{\gamma} &= \sum_{h=0} u_{0}^{(h)} e^{jh\vartheta} + \sum_{h=0} \overline{u}_{0}^{(h)} e^{-jh\vartheta} \end{aligned} \tag{5}$$

in which +, –, and 0 denote positive-, negative-, and zero-sequence components, respectively:

$$\begin{aligned} u_{+}^{(h)} &= \tfrac{1}{3}\left(u_{1}^{(h)} + u_{2}^{(h)} e^{-j(h-1)\frac{2}{3}\pi} + u_{3}^{(h)} e^{-j(h-1)\frac{4}{3}\pi} \right) \\ u_{-}^{(h)} &= \tfrac{1}{3}\left(\overline{u}_{1}^{(h)} + \overline{u}_{2}^{(h)} e^{j(h+1)\frac{2}{3}\pi} + \overline{u}_{3}^{(h)} e^{j(h+1)\frac{4}{3}\pi} \right) \\ u_{0}^{(h)} &= \tfrac{1}{6}\left(u_{1}^{(h)} + u_{2}^{(h)} e^{-jh\frac{2}{3}\pi} + u_{3}^{(h)} e^{-jh\frac{4}{3}\pi} \right). \end{aligned} \tag{6}$$

B. Power harmonic content

Given that both voltage and current space vectors can be defined by (5)-(6) on condition that u is replaced with e and i, respectively, it is possible to express the complex power (s) as

$$s = p + jq = \tfrac{3}{2} e_{\alpha\beta} \overline{i}_{\alpha\beta} + 3 e_{\gamma} i_{\gamma} \tag{7}$$

in which p and q denote active and reactive power, respectively. Substituting (5) in (7) yields

$$s = \sum_{h,k=0} \left(s_{\pm}^{(h-k)} e^{\pm j(h-k)\vartheta} + s_{\pm}^{(h+k)} e^{\pm j(h+k)\vartheta} \right) \tag{8}$$

where h and k denote voltage and current HC order, while:

$$\begin{aligned} s_{+}^{(h-k)} &= \tfrac{3}{2} e_{+}^{(h)} \overline{i}_{+}^{(k)} + 3 e_{0}^{(h)} \overline{i}_{0}^{(k)}, \quad s_{-}^{(h-k)} = \tfrac{3}{2} e_{-}^{(h)} \overline{i}_{-}^{(k)} + 3 \overline{e}_{0}^{(h)} i_{0}^{(k)} \\ s_{+}^{(h+k)} &= \tfrac{3}{2} e_{+}^{(h)} \overline{i}_{-}^{(k)} + 3 e_{0}^{(h)} i_{0}^{(k)}, \quad s_{-}^{(h+k)} = \tfrac{3}{2} e_{-}^{(h)} \overline{i}_{+}^{(k)} + 3 \overline{e}_{0}^{(h)} \overline{i}_{0}^{(k)}. \end{aligned} \tag{9}$$

Focusing on (8), this reveals that a generic pair (h,k) generally leads to two rotating and two counterrotating power space vectors, whose harmonic order are (h–k) and (h+k). Consequently, different power harmonic contents can be achieved depending on number and order of voltage and current HCs, as well as on their sequence components (i.e. positive-, negative- and/or zero-sequence).

III. POWER HARMONIC COMPENSATION

A. General guidelines

Given (7)-(8), active and reactive power can be expressed separately as:

$$\begin{aligned} p &= \tfrac{1}{2}\left(s + \overline{s} \right) = \sum_{h,k=0} \left(p_{\pm}^{(h-k)} e^{\pm j(h-k)\vartheta} + p_{\pm}^{(h+k)} e^{\pm j(h+k)\vartheta} \right) \\ q &= \tfrac{1}{2j}\left(s - \overline{s} \right) = \sum_{h,k=0} \left(q_{\pm}^{(h-k)} e^{\pm j(h-k)\vartheta} + q_{\pm}^{(h+k)} e^{\pm j(h+k)\vartheta} \right) \end{aligned} \tag{10}$$

in which:

$$\begin{aligned} p_{+}^{(h-k)} &= \overline{p}_{-}^{(h-k)} = \tfrac{3}{4} e_{+}^{(h)} \overline{i}_{+}^{(k)} + \tfrac{3}{4} \overline{e}_{-}^{(h)} i_{-}^{(k)} + 3 e_{0}^{(h)} \overline{i}_{0}^{(k)} \\ p_{+}^{(h+k)} &= \overline{p}_{-}^{(h+k)} = \tfrac{3}{4} e_{+}^{(h)} \overline{i}_{-}^{(k)} + \tfrac{3}{4} \overline{e}_{-}^{(h)} i_{+}^{(k)} + 3 e_{0}^{(h)} i_{0}^{(k)} \\ q_{+}^{(h-k)} &= -\overline{q}_{-}^{(h-k)} = \tfrac{3}{4j}\left(e_{+}^{(h)} \overline{i}_{+}^{(k)} - \overline{e}_{-}^{(h)} i_{-}^{(k)} \right) \\ q_{+}^{(h+k)} &= -\overline{q}_{-}^{(h+k)} = \tfrac{3}{4j}\left(e_{+}^{(h)} \overline{i}_{-}^{(k)} - \overline{e}_{-}^{(h)} i_{+}^{(k)} \right). \end{aligned} \tag{11}$$

Considering either (8) or (10), two main cases can be identified, as highlighted in Table I and pointed out in the following:

- when $h = k$, the corresponding power harmonic content is limited to ±(h+k), while a constant power component can be achieved;
- when $h \neq k$, both low-frequency and high-frequency power HCs occur, namely ±(h–k) and ±(h+k), while no constant power is achieved.

As the voltage is generally given, the collection H that groups all the h indexes should be known "a priori". Consequently, the collection K that groups all the k indexes can be defined to suppress or mitigate the power harmonic content. In this regard, the following considerations should be taken into account:

- three independent variables are available for each injected current HC, namely i_{+}, i_{-}, and i_{0};
- ensuring reference active and reactive powers reduces the number of independent variables by one;
- suppressing a power HC completely, i.e. from both p and q, results into two constraints as both positive- and negative-sequence should be compensated for, while suppressing a power HC from just p or q requires a single constraint;
- increasing the number of current HCs slowly increases power harmonic compensation capability because it also increases the number and order of power HCs to compensate for.

The general guidelines introduced above can be clarified further by an explanatory example, namely by assuming H = {1,2}. In this case, choosing K = {1} would lead to just three current phasors in the face of seven power harmonic space vectors (0,±1, ±2, ±3), as shown in Table I. Therefore, power harmonic compensation would be significantly overdetermined, namely just one over the three undesired power HC can be fully suppressed. Alternatively, two over three power HCs could be removed from either p or q, thus full power harmonic compensation is totally prevented.

Still assuming H = {1,2}, different considerations apply by choosing K = {1,2}. In this case, even if the number of power space vectors increases from seven to nine (0,±1, ±2, ±3, ±4), the number of independent variables increases more (from three to six). Consequently, five over eight undesired power harmonic space vectors can be fully suppressed or, more important, a full power harmonic compensation can be achieved on either p or q.

Still assuming H = {1,2}, increasing the number of current HCs beyond $h_{max} = 2$ brings additional benefits, as detectable from Table I. In particular, choosing K = {1,2,3,4,5} leads to fifteen current phasors in the face of fifteen power harmonic

TABLE I. POWER HARMONIC COMPONENT MAP

h \ k	**0**	**1**	**2**	**3**	**4**	**5**	**6**	**7**	…
0	0	±1	±2	±3	±4	±5	±6	±7	…
1	±1	0,±2	±1,3	±2,4	±3,5	±4,6	±5,7	±6,8	…
2	±2	±1,3	0,±4	±1,5	±2,6	±3,7	±4,8	±5,9	…
3	±3	±2,4	±1,5	0,±6	±1,7	±2,8	±3,9	±4,10	…
4	±4	±3,5	±2,6	±1,7	0,±8	±1,9	±2,10	±3,11	…
5	±5	±4,6	±3,7	±2,8	±1,9	0,±10	±1,11	±2,12	…
6	±6	±5,7	±4,8	±3,9	±2,10	±1,11	0,±12	±1,13	…
7	±7	±6,8	±5,9	±4,10	±3,11	±2,12	±1,13	0,±14	…
…	…	…	…	…	…	…	…	…	…

space vectors (0,±1, ±2, ±3, ±4, ±5, ±6, ±7). Consequently, full power harmonic compensation can be achieved, but current harmonic content would be excessively rich.

Based on the previous considerations, it can be stated that injecting current HCs whose order is higher than h_{max} is not recommended, namely k_{max} should be always less than or equal to h_{max}. Additionally, making $k_{max} = h_{max}$ is generally advisable as the interaction between voltage and current HCs of the same order results in constant power, while additional variables improve power harmonic compensation capability.

B. *Case study: H = {1}, K = {1}*

Substituting $h = 1$ and $k = 1$ in (8) yields:

$$s = \left(s_+^{(0)} + s_-^{(0)}\right) + s_+^{(2)} e^{j2\vartheta} + s_-^{(2)} e^{-j2\vartheta} \tag{12}$$

in which $s_\pm^{(0)}$ and $s_\pm^{(2)}$ can be deduced from (9). Therefore, a full power harmonic compensation requires imposing the following constraints:

$$s_+^{(0)} + s_-^{(0)} = s^* , \quad s_+^{(2)} = s_-^{(2)} = 0 \tag{13}$$

where s^* denotes the reference complex power. Solving (13) leads to the following current phasors:

$$\begin{aligned} i_+^{(1)} &= \tfrac{2}{3} \frac{e_+^{(1)}}{\sigma_{1-} E_{1+}^2} \frac{p^* \sigma_{1-} - jq^* \left(\sigma_{1+} - 2\varepsilon_1\right)}{\sigma_{1+} - \left(\varepsilon_1 + \bar{\varepsilon}_1\right)} \\ \bar{i}_-^{(1)} &= \frac{\bar{e}_-^{(1)}}{e_+^{(1)}} i_+^{(1)} = \tfrac{2}{3} \frac{\bar{e}_-^{(1)}}{\sigma_{1-} E_{1+}^2} \frac{p^* \sigma_{1-} - jq^* \left(\sigma_{1+} - 2\varepsilon_1\right)}{\sigma_{1+} - \left(\varepsilon_1 + \bar{\varepsilon}_1\right)} \\ i_0^{(1)} &= -\tfrac{1}{2} \frac{\bar{e}_-^{(1)}}{e_0^{(1)}} i_+^{(1)} = -\tfrac{1}{3} \frac{\bar{\varepsilon}_1}{\sigma_{1-} \bar{e}_0^{(1)}} \frac{p^* \sigma_{1-} - jq^* \left(\sigma_{1+} - 2\varepsilon_1\right)}{\sigma_{1+} - \left(\varepsilon_1 + \bar{\varepsilon}_1\right)} \end{aligned} \tag{14}$$

in which:

$$E_{1\pm} = \left| e_\pm^{(1)} \right| , \quad \sigma_{1\pm} = 1 \pm \frac{E_{1-}^2}{E_{1+}^2} , \quad \varepsilon_1 = \frac{e_-^{(1)} e_0^{(1)}}{e_+^{(1)} \bar{e}_0^{(1)}} . \tag{15}$$

Considering (14), it is worth highlighting that this does not hold in some cases, e.g. i_0 is undefined when e_0 equals zero because it does not contribute to any power component in accordance with (7). Consequently, the number of independent variables reduces (from three to two) and, thus, a full power harmonic compensation is prevented. Similarly, when $E_{1+} = E_{1-}$, σ_{1-} nullifies, making (14) not applicable further; this means that (13) does not have any valid solution, thus a full power harmonic compensation cannot be achieved.

Different considerations can be made when compensating for p HCs only. Particularly, (13) is replaced with:

$$s_+^{(0)} + s_-^{(0)} = s^* , \quad s_+^{(2)} = -\bar{s}_-^{(2)} . \tag{16}$$

As just two constraints occur in face of three current phasors, the problem is underdetermined. Therefore, by nullifying the zero-sequence current phasor for the sake of simplicity, the following solution can be achieved:

$$\begin{aligned} i_0^{(1)} &= 0 , \quad i_+^{(1)} = \tfrac{2}{3} \frac{e_+^{(1)}}{E_{1+}^2} \frac{\left(p^* \sigma_{1+} - jq^* \sigma_{1-}\right)}{\sigma_{1-} \sigma_{1+}} \\ \bar{i}_-^{(1)} &= -\frac{\bar{e}_-^{(1)}}{e_+^{(1)}} i_+^{(1)} = -\tfrac{2}{3} \frac{\bar{e}_-^{(1)}}{E_{1+}^2} \frac{\left(p^* \sigma_{1+} - jq^* \sigma_{1-}\right)}{\sigma_{1-} \sigma_{1+}} . \end{aligned} \tag{17}$$

It is worth noting that also (17) does not hold when $E_{1+} = E_{1-}$ as σ_{1-} nullifies.

C. *General procedure*

The method presented for the case study can be applied to any (H,K) combination, namely an extension of either (13) or (16) can be imposed to achieve a linear system of equations, whose variables are the current phasors. Solving that system results in defining reference current phasors like those expressed by either (14) or (17). Regarding the latter, i_0 does not necessarily need to be nullified, e.g. it can be set suitably to minimize phase current magnitudes. In some cases, overdetermined or underdetermined linear systems could be achieved: the former can be solved by reducing the number of power HCs to compensate for, whereas the latter results in choosing some current phasors in accordance with additional criteria, e.g. equation simplifications or further optimisation targets.

IV. Control System Design

Once the reference currents have been defined, it is necessary to track them at best by means of a suitable control system. As far as a certain number of current HCs could be concerned, the well-known conventional PI-based current control system in the synchronous dq reference frame does not seem longer suitable because reference dq currents would not be constant. Additionally, as the current to inject can have a wide and dense harmonic spectrum, the employment of resonant controllers does not seem advisable. Decoupling current HCs from each other could seem a viable solution as it would enable a number of PI-based current control loops in appropriate synchronous reference frames. However, such a decoupling would require the employment of low-pass filters, which prevent a perfect decoupling, also introducing unsuitable delays that impair control system dynamic performance.

Given the previous considerations, a deadbeat predictive current control approach seems the most suitable choice to implement the proposed PHCS [14]. This is because this control technique can be applied in the αβ stationary reference frame, thus it is able to track any reference current profile with appropriate dynamic performance. On the other hand, model-based predictive control techniques suffer from well-known drawbacks, especially they are highly sensitive to model mismatches, parameter variations and uncertainties. However, the latter could be overcome by on-line parameter identification procedures, as the one proposed in [15].

The proposed PHCS, which has been developed based on the setup shown in Fig. 1, is depicted in Fig. 2. In particular, the setup consists of a three-phase power electronic converter supplied by a DC voltage source and coupled to the electric grid through a simple inductive filter. Consequently, the following equation hold:

$$v_x = r\, i_x + L \frac{di_x}{dt} + e_x \tag{18}$$

in which r and L denote phase resistance and equivalent inductance of the filter, while v is the phase voltage. It is worth noting that, given (4), x can denote either one of the three phases {R,S,T} or one of the space vector components {αβγ}.

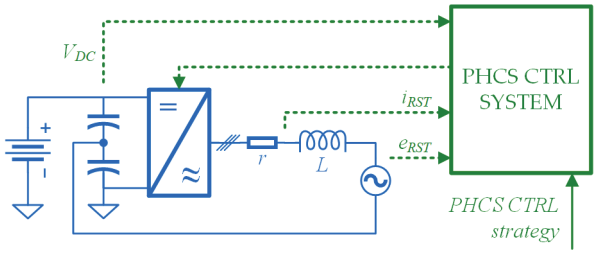

Fig. 1. System setup.

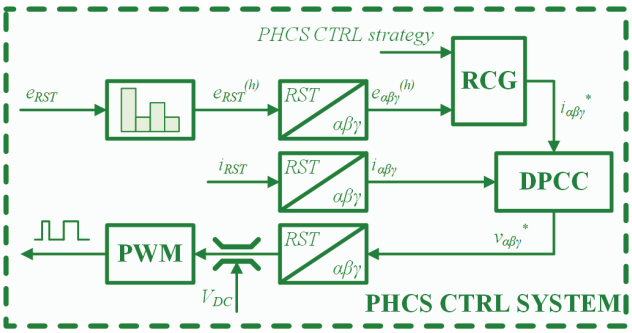

Fig. 2. The proposed PHCS control system: Reference Current Generator (RCG), Deadbeat Predictive Current Control (DPCC), Pulse Width Modulator (PWM).

The exact sample data model of (18) referred to the generic $[k,(k+1)]T_s$ sampling time interval can be thus achieved as

$$i_x^{(k+1)} = f\left(i_x^{(k)} - g e_x^{(k)}\right) + g\sqrt{f}\,v_x^{(k)}, \quad f = e^{-\frac{r}{L}T_s}, \quad g = \frac{T_s}{L} \tag{19}$$

on condition that T_s is sufficiently small compared to r/L and that $1/T_s$ is fairly larger than any HC angular frequency (ω_h) so that the following assumption hold:

$$e^{\left(\frac{r}{L}+j\omega_h\right)T_s} \cong 1 + \left(\frac{r}{L} + j\omega_h\right)T_s \ . \tag{20}$$

Therefore, based on (19), the voltage space vector components can be computed as

$$v_{x,ref}^{(k)} = \frac{1}{g\sqrt{f}}\left(i_{x,ref}^{(k+1)} - f\left(i_x^{(k)} - g e_x^{(k)}\right)\right), \quad x \in \{\alpha,\beta,\gamma\} \ . \tag{21}$$

In conclusion, the corresponding phase voltages can be achieved by inverting (4) and imposing the compliance with the voltage saturation constraint, as highlighted in Fig. 2.

V. Simulations

The effectiveness of the proposed PHCS control system has been verified through a simulation study, which has been carried out in MATLAB-Simulink with reference to the setup shown in Fig. 1, and to the parameters resumed in Table II. Particularly, power system components have been modelled through the Simscape Electrical library, by employing ideal averaged switch models for the DC/AC converter, with a sampling time interval equal to 100 µs. This choice speeds up simulations without impairing their outcomes as switching effects are not relevant to the present study. The proposed PHCS control system is instead modelled through the main Simulink library, and the PWM block shown in Fig. 2 has been replaced with its averaged counterpart. Grid voltages have been set as in Table III, by considering two different cases; in case I, grid voltages consist of 1st-order HCs only (positive-, negative-, and zero-sequence components), whereas 2nd-order HCs have been also included in case II.

Simulations have been carried out by employing three different sets of reference currents sequentially, as pointed out in Table IV. Regardless of the specific case, 1st-order positive-sequence reference currents have been used first (cases I.A and II.A), thus ignoring any higher-order voltage HCs, as well as negative- and zero-sequence voltage components. Subsequently (cases I.B and II.B), reference currents have been imposed in accordance with (14), namely to fully suppress as many power HCs as possible. This requires excessive zero-sequence current HCs, as detectable from Table IV, hardly achievable in practice. However, it is worth noting that such a large zero-sequence current HC derives from weak zero-sequence voltage HCs (Table III). Therefore, much smaller zero-sequence current HCs could be achieved in case of more significant zero-sequence voltage HCs. Last (cases I.C and II.C), reference currents have been set in accordance with (17) to suppress HCs from active power only. However, in case II.C, the zero-sequence current component has been set different from zero to mitigate phase current magnitude. Table IV reveals that, differently from the previous cases (I.B and II.B), much less significant zero-sequence current HCs are required, making this strategy more feasible to implement in practice.

Simulation results are reported from Fig. 3 to Fig. 10, while HC magnitudes and Total Harmonic Distortion (THD) values are resumed in Table V and Table VI, respectively. Focusing on case I first, Fig. 4 confirms what expected, namely excessive current magnitudes are required to fully suppress HCs from both active and reactive powers (case I.B). These current evolutions are also quite similar to each other as they are predominated by the zero-sequence component, as pointed out in Table IV. This control strategy leads also to significant power fluctuations in each phase (Fig. 5), although it succeeds in suppressing power HCs completely (Fig. 6). It is worth noting that the proposed deadbeat current control algorithm ensures a good tracking of the reference current profiles as the active power dip occurring at 60 ms is due to unoptimized voltage saturation management only. Much better results are achieved when compensating for active power HCs only (case I.C), namely current magnitudes decreased significantly, becoming quite similar to those achieved in case I.A, although reactive power ripple increases.

Similar considerations can be made with reference to case II, although some differences occur. Since a full PHCS is prevented in accordance with what stated in Section III, suppressing low-order power HCs (1st and 2nd on p and q, also 3rd on p) increases 4th-order power HC and ripple unsuitably (case II.B, Fig. 10). Better results are achieved by compensating for active power HCs only (case II.C), although current magnitudes and phase power fluctuations seem still excessive (Fig. 8 and Fig. 9, respectively).

TABLE II. Simulation Parameters and Rated Values

Symbol	V_{DC}	r	L	E_n	f_n	I_n	P_n
Value	1000	1	850	230	50	10	4.88
Unit	V	mΩ	µF	V_{rms}	Hz	A	kW

TABLE III. Grid Voltage HCs[a]

	$e_+^{(1)}$		$e_-^{(1)}$		$e_0^{(1)}$		$e_+^{(2)}$		$e_-^{(2)}$		$e_0^{(2)}$	
	|·|	∟	|·|	∟	|·|	∟	|·|	∟	|·|	∟	|·|	∟
case I	1.00	0	0.05	1.17	0.01	0	-	-	-	-	-	-
case II							0.02	0	0.05	0.25	0.01	0

[a] Voltage magnitudes are in per unit (base voltage = 230 V_{rms}, base angle = π)

TABLE IV. Reference Current Phasors[b]

	$i_+^{(1)}$		$i_-^{(1)}$		$i_0^{(1)}$		$i_+^{(2)}$		$i_-^{(2)}$		$i_0^{(2)}$	
case	|·|	∟	|·|	∟	|·|	∟	|·|	∟	|·|	∟	|·|	∟
I.A	1.12	–0.15	-	-	-	-	-	-	-	-	-	-
I.B	1.07	–0.16	0.05	–0.68	2.67	–0.32	-	-	-	-	-	-
I.C	1.12	–0.15	0.06	0.31	-	-	-	-	-	-	-	-
II.A	1.12	–0.15	-	-	-	-	-	-	-	-	-	-
II.B	1.16	–0.14	0.06	–0.69	2.91	–0.31	0.03	–0.01	0.24	–0.46	3.75	–0.79
II.C	1.15	–0.14	0.08	0.24	0.73	0.90	0.00	0.25	0.05	–0.45	0.03	–0.61

[b] Current magnitudes and angles are in per unit (base current = 10 A, base angle = π)

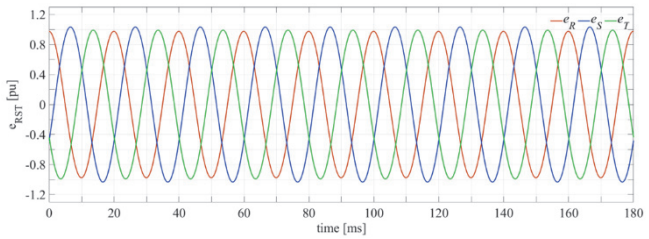

Fig. 3. Emf evolutions achieved in case I: I.A (from 0 to 60 ms), I.B (from 60 to 120 ms), and I.C (from 120 to 180 ms).

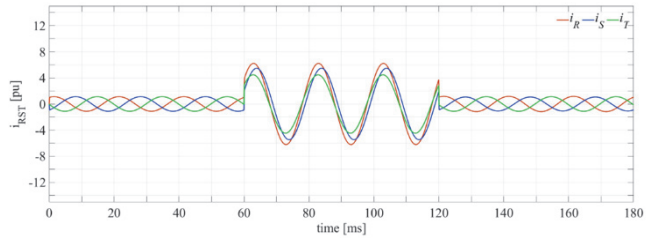

Fig. 4. Current evolutions achieved in case I: I.A (from 0 to 60 ms), I.B (from 60 to 120 ms), and I.C (from 120 to 180 ms).

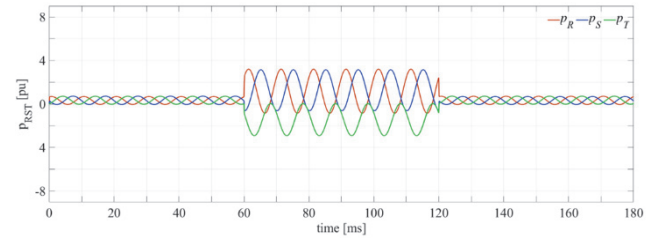

Fig. 5. Power evolutions achieved in case I: I.A (from 0 to 60 ms), I.B (from 60 to 120 ms), and I.C (from 120 to 180 ms).

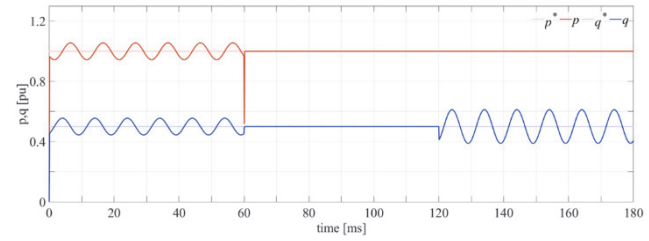

Fig. 6. Active and reactive power evolutions achieved in case I: I.A (from 0 to 60 ms), I.B (from 60 to 120 ms), and I.C (from 120 to 180 ms).

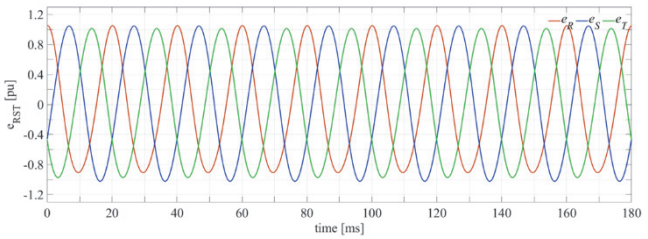

Fig. 7. Emf evolutions achieved in case II: II.A (from 0 to 60 ms), II.B (from 60 to 120 ms), and II.C (from 120 to 180 ms).

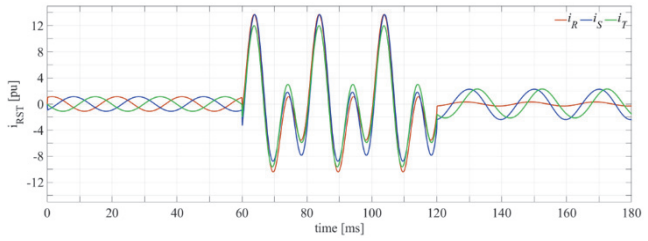

Fig. 8. Current evolutions achieved in case II: II.A (from 0 to 60 ms), II.B (from 60 to 120 ms), and II.C (from 120 to 180 ms).

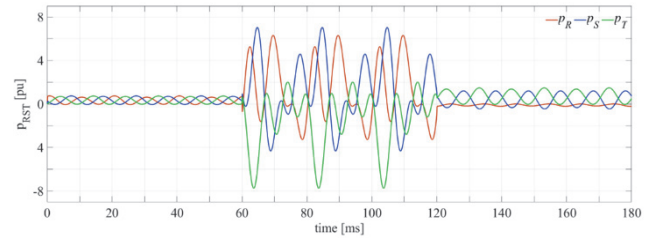

Fig. 9. Power evolutions achieved in case II: II.A (from 0 to 60 ms), II.B (from 60 to 120 ms), and II.C (from 120 to 180 ms).

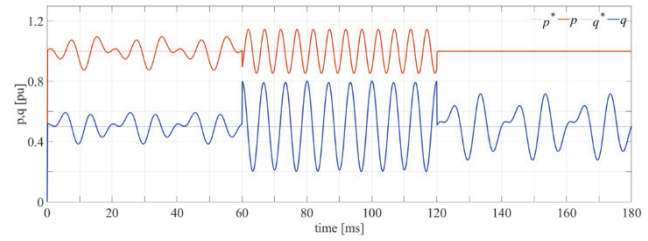

Fig. 10. Active and reactive power evolutions achieved in case II: II.A (from 0 to 60 ms), II.B (from 60 to 120 ms), and II.C (from 120 to 180 ms).

TABLE V. HC MAGNITUDES[c]

Case	I.A			I.B			I.C			II.A					II.B					II.C				
HC	*0*	*1st*	*2nd*	*0*	*1st*	*2nd*	*0*	*1st*	*2nd*	*0*	*1st*	*2nd*	*3rd*	*4th*	*0*	*1st*	*2nd*	*3rd*	*4th*	*0*	*1st*	*2nd*	*3rd*	*4th*
e_R	-	0.98	-	-	0.98	-	-	0.98	-	-	0.98	0.08	-	-	-	0.98	0.08	-	-	-	0.98	0.08	-	-
e_S	-	1.03	-	-	1.03	-	-	1.03	-	-	1.03	0.04	-	-	-	1.03	0.04	-	-	-	1.03	0.04	-	-
e_T	-	0.99	-	-	0.99	-	-	0.99	-	-	0.99	0.04	-	-	-	0.99	0.04	-	-	-	0.99	0.04	-	-
i_R	-	1.12	-	-	6.22	-	-	1.17	-	-	1.12	-	-	-	-	6.80	7.31	-	-	-	0.31	0.01	-	-
i_S	-	1.12	-	-	5.47	-	-	1.07	-	-	1.12	-	-	-	-	5.97	7.76	-	-	-	2.32	0.09	-	-
i_T	-	1.12	-	-	4.47	-	-	1.12	-	-	1.12	-	-	-	-	4.88	7.44	-	-	-	2.21	0.08	-	-
p_R	0.32	-	0.36	1.17	-	2.03	0.33	-	0.38	0.32	0.03	0.36	0.03	-	1.28	2.20	2.21	2.46	0.20	0.10	0.01	0.10	0.01	-
p_S	0.34	-	0.39	1.26	-	1.89	0.32	-	0.37	0.34	0.01	0.39	0.01	-	1.20	2.61	2.06	2.65	0.10	0.40	0.03	0.80	0.03	-
p_T	0.34	-	0.37	1.44	-	1.48	0.35	-	0.37	0.34	0.01	0.37	0.01	-	1.48	2.43	1.62	2.41	0.10	0.69	0.02	0.73	0.04	-
p	1.00	-	0.06	1.00	-	-	1.00	-	-	1.00	0.02	0.06	0.06	-	1.00	-	-	-	0.15	1.00	-	-	-	-
q	0.50	-	0.06	0.50	-	-	0.50	-	0.11	0.50	0.02	0.06	0.06	-	0.50	-	-	0.30	0.01	0.50	0.02	0.14	0.1	-

[c] All magnitudes are in per unit (base voltage = 230 V_{rms}, base current = 10 A, base power = 4.88 kW-kVAR)

TABLE VI. THDs (PU)

	I.A	I.B	I.C	II.A	II.B	II.C
$\mathbf{e_R}$	-	-	-	0.09	0.09	0.09
$\mathbf{e_S}$	-	-	-	0.04	0.04	0.04
$\mathbf{e_T}$	-	-	-	0.04	0.04	0.04
$\mathbf{i_R}$	-	-	-	-	1.08	0.02
$\mathbf{i_S}$	-	-	-	-	1.30	0.04
$\mathbf{i_T}$	-	-	-	-	1.52	0.04
$\mathbf{p_R}$	1.13	1.73	1.15	1.14	3.10	1.05
$\mathbf{p_S}$	1.14	1.49	1.16	1.14	3.54	1.99
$\mathbf{p_T}$	1.08	1.03	1.06	1.09	2.55	1.06
p	0.06	-	-	0.08	0.15	-
q	0.11	-	0.22	0.16	0.59	0.34

In conclusion, THD has been computed for each voltage, current, and power, whose values are reported in Table VI. In this regard, it is worth noting that, differently from voltages and currents, the power THD has been computed with reference to the zero-order instead of to the 1st-order HC. The THD values confirm that cases I.B and II.B result in excessive power and/or current distortion, while much better results are achieved in cases I.C and II.C. Particularly, active power HCs can be fully suppressed in case II.C at the cost of slightly increasing current THD (2-4%) and, to a more extent, reactive power ripple.

VI. Conclusion

A current control system that defines and tracks reference currents to suppress power Harmonic Components (HCs) in either electric drives or grid-connected power electronic converters has been presented in this paper. The proposed method can be applied in case of any three-phase electro-motive force, especially those characterized by multiple sequence and/or harmonic components. Simulation results, which refer to two different scenarios, confirm the validity of the proposed theoretical analysis, but showing some eventual limitations. Particularly, it has been shown that suppressing HCs from both active and reactive powers may require excessive zero-sequence current HCs, leading to unfeasible current magnitudes and distortion. On the other hand, suppressing HCs from active power only seems a more promising solution, although it comes at the cost of increased current distortion. In the light of the results shown in the paper, the definition of a sound guideline on this topic requires further and more extensive studies, especially by considering a large number of HCs so that the proposed method can be generalised and assessed successfully. This will be investigated in the incoming future, and the corresponding results will be presented in future works.

Acknowledgment

This work was partially supported by “Convenzione triennale tra la Fondazione di Sardegna e gli Atenei Sardi - Regione Sardegna L.R.7/2007 annualità 2019-DGR DGR 28/21 del 17.05.2015” with project “Formal Methods and Technologies for the Future of Energy Systems”, CUP F72F20000350007, call 2019.

References

[1] M. P. Kazmierkowski and L. Malesani, “Current control techniques for three-phase voltage-source PWM converters: a survey,” *IEEE Trans. Ind. Electron.*, vol. 45, no. 5, pp. 691–703, Oct. 1998, doi: 10.1109/41.720325.

[2] Z. Hu, Y. Han, A. S. Zalhaf, S. Zhou, E. Zhao, and P. Yang, “Harmonic Sources Modeling and Characterization in Modern Power Systems: A Comprehensive Overview,” *Electr. Power Syst. Res.*, vol. 218, p. 109234, May 2023, doi: 10.1016/j.epsr.2023.109234.

[3] Q. Liu, F. Liu, Y. Li, and S. Wang, “Harmonic modeling and harmonic contribution determination: A case study of industrial power supply system,” *Electr. Power Syst. Res.*, vol. 217, p. 109122, Apr. 2023, doi: 10.1016/j.epsr.2023.109122.

[4] K. U. Vinayaka and P. S. Puttaswamy, “Analysis of current harmonics compensation using various active filter topologies,” *Mater. Today Proc.*, vol. 58, pp. 580–586, Jan. 2022, doi: 10.1016/j.matpr.2022.03.411.

[5] J. Miret, M. Castilla, A. Camacho, L. G. de Vicuña, and J. Matas, “Control Scheme for Photovoltaic Three-Phase Inverters to Minimize Peak Currents During Unbalanced Grid-Voltage Sags,” *IEEE Trans. Power Electron.*, vol. 27, no. 10, pp. 4262–4271, Oct. 2012, doi: 10.1109/TPEL.2012.2191306.

[6] Y. W. Li and J. He, “Distribution System Harmonic Compensation Methods: An Overview of DG-Interfacing Inverters,” *IEEE Ind. Electron. Mag.*, vol. 8, no. 4, pp. 18–31, Dec. 2014, doi: 10.1109/MIE.2013.2295421.

[7] H. Eroğlu, E. Cuce, P. Mert Cuce, F. Gul, and A. Iskenderoğlu, “Harmonic problems in renewable and sustainable energy systems: A comprehensive review,” *Sustain. Energy Technol. Assess.*, vol. 48, p. 101566, Dec. 2021, doi: 10.1016/j.seta.2021.101566.

[8] N. Patel, A. Elnady, R. C. Bansal, A.-K. Hamid, and A. A. Adam, “A novel proposal for harmonic compensation in the grid-connected photovoltaic system under electric anomalies,” *Electr. Power Syst. Res.*, vol. 223, p. 109512, Oct. 2023, doi: 10.1016/j.epsr.2023.109512.

[9] J.-K. Kim, J.-H. Lee, H.-G. Jeong, and K.-B. Lee, “Improvement of grid-connected inverter systems with PR controllers under the unbalanced and distorted grid voltage,” in *Proceedings of The 7th International Power Electronics and Motion Control Conference*, Jun. 2012, pp. 1183–1187. doi: 10.1109/IPEMC.2012.6258998.

[10] W. Jiang, Y. Wang, J. Wang, L. Wang, and H. Huang, “Maximizing Instantaneous Active Power Capability for PWM Rectifier Under Unbalanced Grid Voltage Dips Considering the Limitation of Phase Current,” *IEEE Trans. Ind. Electron.*, vol. 63, no. 10, pp. 5998–6009, Oct. 2016, doi: 10.1109/TIE.2016.2577544.

[11] P. Rodriguez, A. V. Timbus, R. Teodorescu, M. Liserre, and F. Blaabjerg, “Flexible Active Power Control of Distributed Power Generation Systems During Grid Faults,” *IEEE Trans. Ind. Electron.*, vol. 54, no. 5, pp. 2583–2592, Oct. 2007, doi: 10.1109/TIE.2007.899914.

[12] Y. Song and H. Nian, “Stationary frame control strategy for voltage source inverter under unbalanced and distorted grid voltage,” in *2014 IEEE Energy Conversion Congress and Exposition (ECCE)*, Sep. 2014, pp. 1167–1173. doi: 10.1109/ECCE.2014.6953532.

[13] Y. Quan, H. Nian, and N. S. Yu, “A novel approach to obtain constant DC-link voltage of the grid-connected converter under harmonically grid voltage conditions,” in *2011 International Conference on Electrical Machines and Systems*, Aug. 2011, pp. 1–6. doi: 10.1109/ICEMS.2011.6073382.

[14] P. Cortes, M. P. Kazmierkowski, R. M. Kennel, D. E. Quevedo, and J. Rodriguez, “Predictive Control in Power Electronics and Drives,” *IEEE Trans. Ind. Electron.*, vol. 55, no. 12, pp. 4312–4324, Dec. 2008, doi: 10.1109/TIE.2008.2007480.

[15] G. Gatto, I. Marongiu, and A. Serpi, “Discrete-Time Parameter Identification of a Surface-Mounted Permanent Magnet Synchronous Machine,” *IEEE Trans. Ind. Electron.*, vol. 60, no. 11, pp. 4869–4880, Nov. 2013, doi: 10.1109/TIE.2012.2221113.